methods

Quantification of sterol lipids in plants by quadrupole time-of-flight mass spectrometry

Vera Wewer, Isabel Dombrink, Katharina vom Dorp, and Peter Dörmann[1]

Institute of Molecular Physiology and Biotechnology of Plants, University of Bonn, 53115 Bonn, Germany

Abstract **Glycerolipids, sphingolipids, and sterol lipids constitute the major lipid classes in plants. Sterol lipids are composed of free and conjugated sterols, i.e., sterol esters, sterol glycosides, and acylated sterol glycosides. Sterol lipids play crucial roles during adaption to abiotic stresses and plant-pathogen interactions. Presently, no comprehensive method for sterol lipid quantification in plants is available. We used nanospray ionization quadrupole-time-of-flight mass spectrometry (Q-TOF MS) to resolve and identify the molecular species of all four sterol lipid classes from *Arabidopsis thaliana*. Free sterols were derivatized with chlorobetainyl chloride. Sterol esters, sterol glycosides, and acylated sterol glycosides were ionized as ammonium adducts. Quantification of molecular species was achieved in the positive mode after fragmentation in the presence of internal standards. The amounts of sterol lipids quantified by Q-TOF MS/MS were validated by comparison with results obtained with TLC/GC. Quantification of sterol lipids from leaves and roots of phosphate-deprived *A. thaliana* plants revealed changes in the amounts and molecular species composition. The Q-TOF method is far more sensitive than GC or HPLC. Therefore, Q-TOF MS/MS provides a comprehensive strategy for sterol lipid quantification that can be adapted to other tandem mass spectrometers.**—Wewer, V., I. Dombrink, K. vom Dorp, and P. Dörmann. **Quantification of sterol lipids in plants by quadrupole time-of-flight mass spectrometry. *J. Lipid Res.* 2011.** 52: **1039–1054.**

Supplementary key words *Arabidopsis* • campesterol • cholesterol • phosphate limitation • phytosterol • sitosterol • stigmasterol

Glycoglycerolipids (monogalactosyl diacylglycerol, digalactosyl diacylglycerol [DGDG], and sulfolipid [SQDG]) are the most abundant membrane lipids in chloroplasts of plants (1, 2). Different lipid classes, however, are prevalent in extraplastidial membranes. Phosphoglycerolipids (e.g., phosphatidylcholine and phosphatidylethanolamine) are abundant constituents of the plasma membrane, the tonoplast, and the endoplasmic reticulum. Furthermore, sphingolipids, in particular glucosylceramides and glycosylinositolphosphoceramides, are present in extraplastidial membranes of plants (3, 4). In addition to glycerolipids and sphingolipids, sterol lipids represent the third membrane lipid class in plants. In contrast to animals and yeast, where cholesterol and ergosterol, respectively, are prevalent, phytosterols (campesterol, stigmasterol, and sitosterol) represent the most abundant sterols in plants (5). The biosynthetic pathway for phytosterols also provides the precursors for brassinosteroids, phytohormones involved in the regulation of plant growth and development (6).

Free sterols (FS) with a nonconjugated 3-hydroxy group are found in the plasma membrane and other extraplastidial membranes of plant cells. In addition, different classes of conjugated sterols are found in plants, sterol ester (SE), sterol glucoside (SG), and acylated (esterified) sterol glucoside (ASG). Plant cells contain considerable amounts of SEs, which in contrast to the other sterol lipid classes, are localized to the oil bodies of the cytosol (7, 8). Oil bodies are the sites of lipid storage and contain large amounts of triacylglycerol and SEs. Two acyltransferases were identified in *Arabidopsis*, acyl-CoA:sterol acyltransferase and phospholipid:sterol acyltransferase (PSAT), capable of transferring acyl groups from acyl-CoA or from a phosphoglycerolipid, respectively, onto the 3-hydroxy group of sterols (9, 10). A deficiency in PSAT activity causes early leaf senescence, and it is believed that acylation of sterols is crucial for the regulation of the FS content in plant membranes (11).

SGs carry a D-glucose in β-glycosidic linkage of the 3-hydroxy group of the sterol (12, 13). The first gene encoding sterol glucosyltransferase was isolated from oat (14). Two

This work was supported by an Instrument grant (Forschungsgrossgeräte-Antrag) and by the Forschungsschwerpunkt 1212 of Deutsche Forschungsgemeinschaft (grant Do520/9).

Manuscript received 6 January 2011 and in revised form 14 February 2011.

Published, JLR Papers in Press, March 7, 2011
DOI 10.1194/jlr.D013987

Abbreviations: ASG, acylated sterol glucoside; DGDG, digalactosyl diacylglycerol; DW, dry weight; FAG, acyl-glucoside-specific fragment; FB, betainyl fragment; F_S, sterol-specific fragments; FS, free sterol; FW, fresh weight; Glc, glucose; MS/MS, tandem mass spectrometry; PSAT, phospholipid-sterol acyltransferase; Q-TOF, quadrupole time-of flight; SE, sterol ester; SG, sterol glucoside; SPE, solid phase extraction; SQDG, sulfolipid; WT, wild type.

[1]To whom correspondence should be addressed.
e-mail: doermann@uni-bonn.de

genes encoding sterol glucosyltransferases are present in *Arabidopsis*. A mutant line carrying insertions in the two *Arabidopsis* genes is affected in seed coat formation and suberization (15). Acylation with a long chain fatty acid at position 6 of the glucose moiety results in the formation of ASG (16). SGs and ASGs are found in the plasma membrane of plants and some yeast species (17). Sterol lipids are believed to contribute to diverse functions in the plant cell. Different forms of sterols are involved in plant–pathogen interactions. A recent study showed that in *Arabidopsis*, sitosterol is converted into stigmasterol during *Pseudomonas* infection (18). Furthermore, sterol glucosides play important roles during the immune response in humans after *Helicobacter* infection and in peroxisome degradation in *Pichia* (19, 20).

Recently, the role of phosphate availability for glycerolipid metabolism has been studied in great detail. Phosphate deprivation results in the replacement of a large proportion of phosphoglycerolipids with DGDG and SQDG to save phosphate for other important cellular processes (2, 21). This alteration in membrane lipid composition is associated with an upregulation of the expression of the biosynthetic genes for DGDG and SQDG, demonstrating that this adaptive process is regulated via activation of gene expression. The role of other glycolipids during phosphate deficiency, including SGs and ASGs, is less well understood. ASGs were found to be particularly increased in detergent-insoluble membranes of oat root plasma membranes during phosphate deprivation (22). At present, no data for the molecular species composition of SEs and of ASGs during normal conditions or phosphate deprivation are available.

Due to the presence of a large number of molecular species, the measurement of the different sterol lipids in plants is challenging. Previously, membrane lipids, including sterols, were separated by HPLC via normal phase chromatography coupled with evaporative light scattering detection (23, 24). However, this approach is hampered by a limitation in sensitivity and linearity of the detector signal. Furthermore, no information on molecular species composition can be obtained. An alternative approach includes the separation and isolation of different sterol lipid classes via TLC and the quantification of the sterol moieties by GC after hydrolyzation (11, 15, 22). This strategy provides data on the sterol composition of sterol lipid classes but not on the composition of individual molecular species of SEs and ASGs. Furthermore, two different TLC systems are required to separate the polar (SG and ASG) and the nonpolar sterol lipids (FS and SE). In addition, this method is labor intensive and suffers from a lack of sensitivity.

Recently, the availability of high-resolution mass spectrometers has resulted in the development of highly sensitive and accurate methods for the identification and quantification of lipids (25). Phosphoglycerolipids and glycoglycerolipids can be measured in total leaf lipid extracts by direct infusion ESI coupled with triple quadrupole mass spectrometry (MS) (26, 27). In this strategy, the masses of the individual molecular lipid species are selected by the first quadrupole, and, after fragmentation, the lipids are quantified using characteristic fragmentation patterns (neutral loss or precursor ion scanning). The separation of lipids via HPLC coupled with a quadrupole ion trap (Q-trap) mass spectrometer was employed for the quantification of plant sphingolipids (3, 4). After separation by HPLC, the sphingolipids are quantified via multiple reaction monitoring, taking advantage of the characteristic mass transitions after fragmentation. An alternative strategy, i.e., direct infusion quadrupole time-of-flight MS (Q-TOF MS) was applied to the quantitative analysis of yeast lipids including phospholipids, sphingolipids, triacylglycerol, and diacylglycerol (28). A number of methods were recently developed for the analysis of cholesterol, oxysterols, and related sterols from animals or humans by LC or ESI-MS (29–33). Thus, free sterols were usually derivatized to improve ionization, and derivatized FSs and SEs were analyzed in tandem MS (MS/MS) experiments. However, for plants, no comprehensive method for sterol lipid analysis was developed.

The goal of the present study was to establish a method for the detection, identification, and quantification of the different molecular species of all four sterol lipid classes in plants by employing nanospray ionization Q-TOF MS/MS.

EXPERIMENTAL PROCEDURES

Plants and growth conditions

Arabidopsis thaliana, ecotype Columbia-0, was grown in pots in a mixture of soil and vermiculite (2:1) for 4 weeks in phytotrons at 20°C, 8 h of light (150 μmol m^{-2} s^{-1}) per day, and 55% relative humidity. For phosphate deprivation, seedlings were grown on agar-solidified medium containing Murashige and Skoog salts for 2 weeks (34) and then grown on synthetic nutrient medium for an additional 2 weeks (35, 36). The *pho1-2* mutant (37, 38) was obtained from the Nottingham *Arabidopsis* Seed Center (Nottingham, UK). The *pho1-2* mutant (a loss-of function mutant allelic to *pho1-1*) is abbreviated as *pho1* throughout the text.

Lipid standards

Cholestanol and stigmastanol (Sigma) were used as internal standards for the quantification of FSs. Internal standards for the quantification of SEs were 16:0-cholesterol, 16:1-cholesterol, 18:0-cholesterol, and 18:1-cholesterol (fatty acids are abbreviated X:Y, where X represents the number of carbon atoms, and Y represents the number of double bonds in the acyl chain) (Sigma). The SGs used as internal standards were synthesized as described previously (39) using cholestanol and stigmastanol. Briefly, 1.25 g of glucopyranosyl-bromide-tetrabenzoate were dissolved in 10 ml of toluene and added to a suspension of 0.61 g of sterol, 2 g of drierite, and 2 g of $CdCO_3$ in 12 ml of toluene. The mixture was incubated at 130°C for 7 h. After cooling, the suspension was diluted with 24 ml of chloroform and filtered after celite was added. The filtrate was dried under a stream of N_2, resuspended in 40 ml of 0.15 M sodium methylate, and incubated overnight with shaking at room temperature. The solution was neutralized with 1 N methanolic HCl, and the products were extracted with chloroform-methanol (2:1) and water. The SGs were purified by solid phase extraction (SPE) on silica columns (see below) or by TLC and quantified by GC. Acylated (esterified) sterol glucosides from soybean (containing stigmasterol, sitosterol, and campesterol;

Matreya, Pleasant Gap, PA) were hydrogenated with H_2 gas in chloroform in the presence of platinum(IV)oxide as described previously (40). Complete saturation of the acyl and sterol moieties was confirmed by Q-TOF MS/MS analysis. Standard sterol lipids were hydrolyzed with methanolic HCl, and fatty acids were converted into their methyl esters as described below. Fatty acid methyl esters derived from SE and ASG were quantified by GC. The sterol moieties of FS, SG, and ASG were converted into trimethylsilyl ethers and quantified by GC. The standard lipid mixture (in 50 µl of chloroform-methanol, 2:1) contained 5 nmol each of cholestanol and stigmastanol; 2.5 nmol each of 16:0-cholesterol, 18:0-cholesterol, 16:1-cholesterol, and 18:1-cholesterol; 5 nmol each of cholestanol-Glc and stigmastanol-Glc; 0.2 nmol of 16:0-Glc-campestanol; 0.5 nmol of 16:0-Glc-stigmastanol; 0.3 nmol of 18:0-Glc-campestanol; and 1 nmol of 18:0-Glc-stigmastanol.

Extraction of total lipids and SPE

Arabidopsis leaves or roots (20–100 mg fresh weight [FW]) were ground to a fine powder in liquid N_2. Total lipids were extracted with 500 µl of chloroform-methanol-formic acid (1:1:0.1) and 250 µl of a solution of 1 M KCl and 0.2 M H_3PO_4. All organic solvents contained 0.01% butylated hydroxytoluene as antioxidant. The internal standard mixture (50 µl) was added. The sample was vortexed and centrifuged (7,500 *g*, 2 min) to obtain phase separation. The lower, organic phase was harvested with a pipette. Two additional extractions with 250 µl of chloroform-methanol (2:1) each were done, and the organic phases were combined. The solvent was evaporated under a stream of N_2 gas. Nonpolar lipids, glycolipids, and phospholipids were separated by SPE using Strata silica columns (1 ml bed volume; Phenomenex). Lipids were applied to the silica columns in 100% chloroform, and nonpolar lipids (including FS and SE) were eluted with 2 ml of chloroform. The glycolipid fraction containing SG and ASG was obtained by elution with 1 ml of acetone-2-propanol (1:1).The purified lipid extracts containing FS/SE or SG/ASG were dried and dissolved in 1 ml of Q-TOF solvent (see below). FSs were derivatized with *N*-chlorobetainyl chloride prior to Q-TOF analysis (see below).

Quantification of sterol lipids by TLC and GC

Lipids were extracted from leaves (2 g of material) and separated into nonpolar and polar fractions by SPE on silica columns, as described above. The nonpolar fraction containing FS and SE and the polar fraction containing SG and ASG were each divided into two aliquots. One aliquot was used for Q-TOF analysis, and the other aliquot was used for quantification by TLC/SPE and GC (**Fig. 1**). Nonpolar lipids (FS and SE) were separated by an additional step of SPE with a silica column by application to the column in 100% hexane and elution with hexane-diethylether (99:1) (for SE) and hexane-diethylether (85:15) (for FS) (see http://www.cyberlipid.org). For the TLC separation of polar lipids, Baker Si 250 TLC plates (J.T. Baker, Phillipsburg, NJ) were impregnated with 0.15 M ammonium sulfate and activated for 2.5 h at 120°C. The TLC plates were developed in acetone-toluene-water (91:30:8) (41), and lipids were isolated from the silica material with chloroform-methanol (2:1). For GC analysis, SEs were hydrolyzed in 1 ml of 6% (w/v) KOH in methanol at 90°C for 1 h and then extracted with hexane (42). SG and ASG were hydrolyzed in 1 ml of 1 N methanolic HCl at 90°C for 30 min. After the addition of 1 ml of 0.9% NaCl, the hydrolyzed sterols were extracted with 1 ml of hexane. Sterols were derivatized with 100 µl of *N*-methyl-*N*-(trimethylsilyl)-trifluoroacetamide (MSTFA) prior to GC analysis. MSTFA was evaporated in an N_2 gas stream, and the samples were dissolved in hexane. GC analysis was carried out with an Agilent 7890A Plus GC unit with flame ionization detector (Agilent). Silylated sterols were separated on a 30 m HP-5MS column (Agilent) using a temperature gradient of 150°C increased to 280°C at 10°C min^{-1}, held for 10.5 min, and decreased to 150°C at 20°C min^{-1}. Sterols were identified by GC-MS (Agilent) using the same column and temperature gradient.

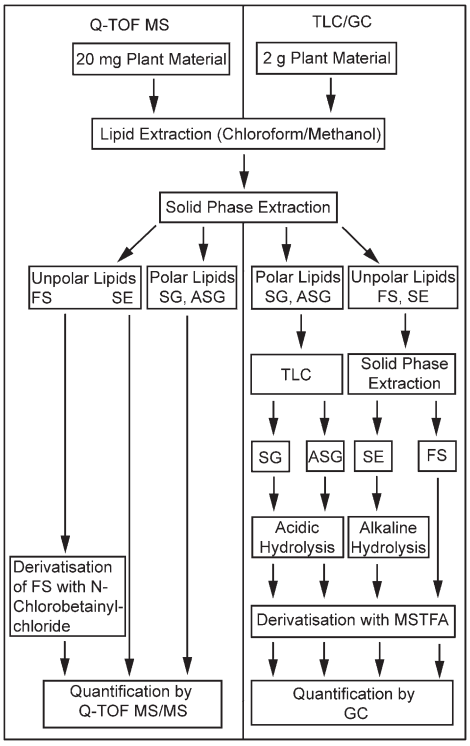

Fig. 1. Flow chart for sterol lipid quantification. Sterol lipids were obtained from ~2 g of leaf material and, after fractionation by TLC and SPE, were quantified by GC. The direct infusion MS strategy is based on lipid extracts obtained from ~20 mg of leaf material. Lipids are fractionated by SPE and quantified by Q-TOF MS/MS.

Derivatization of free sterols for Q-TOF MS/MS

Free sterols were derivatized with *N*-chlorobetainyl chloride following the procedure described for diacylglycerol derivatization (43). Briefly, lipids (nonpolar fraction after SPE purification) were dissolved in 0.5 ml of anhydrous methylene chloride. Then, 50 µl of anhydrous pyridine and 5 mg of *N*-chlorobetainyl chloride (see below) were added, and the sample was incubated at 42°C for 4 h (or overnight with the same results). The betainylated sterols were extracted with 2 vol of chloroform-methanol (1:1) and 1 vol of water. Derivatized sterols were stable for at least 48 h at 18°C (as measured by Q-TOF MS/MS analysis). For the synthesis of *N*-chlorobetainyl chloride, 1 g of betaine hydrochloride was added to 0.93 g of thionyl chloride (44). The mixture was slowly heated to 70°C and incubated overnight. After the addition of 1 ml of warm (~70°C) toluene, the reaction mixture was cooled to room temperature with stirring. More warm toluene was added, and the reaction mixture was heated until the substances were dissolved. After cooling again, crystals formed, which were washed twice with methylene chloride, dried, and stored at 4°C.

Q-TOF MS

Sterols purified by SPE were introduced into the Q-TOF mass spectrometer (Agilent 6530 Accurate Mass Q-TOF LC-MS unit) operated in the positive mode via direct nanospray infusion

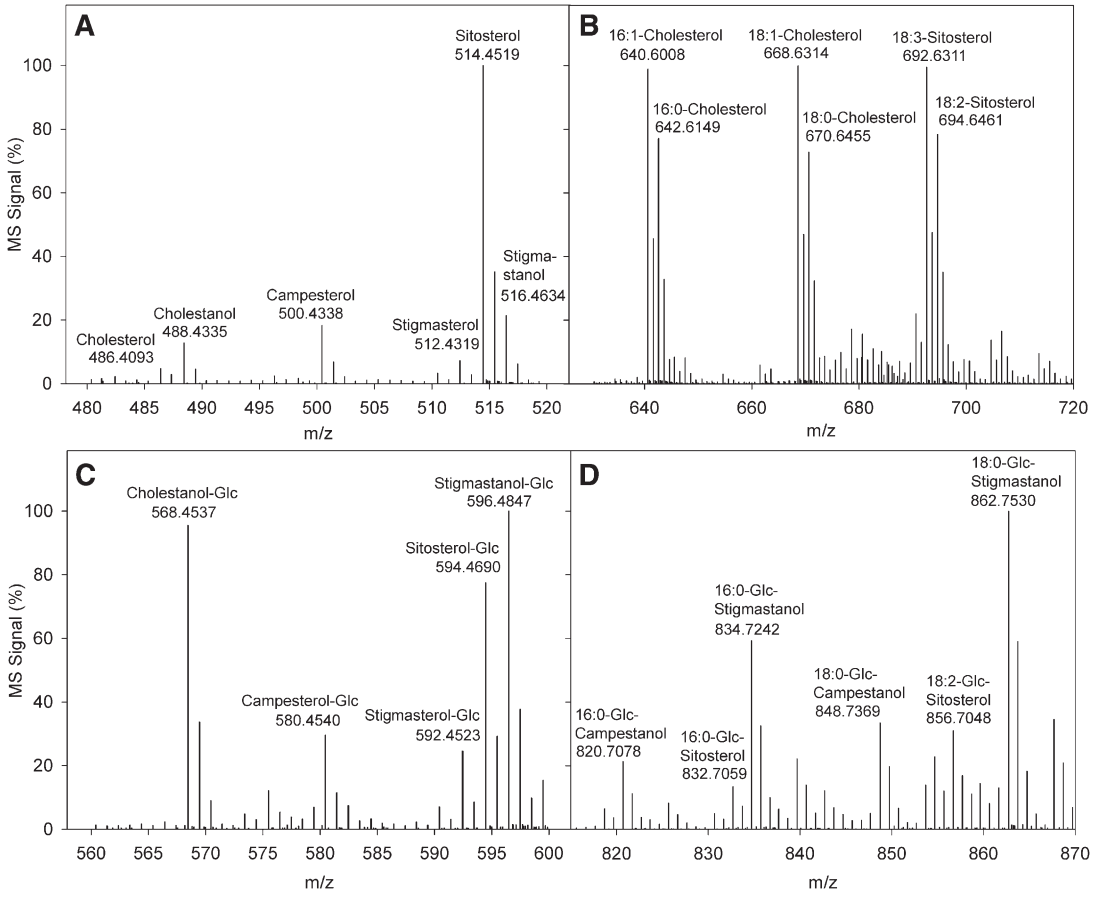

Fig. 2. Mass spectra of sterol lipids without fragmentation. Sterol lipids were directly infused into the Q-TOF mass spectrometer via nanospray ionization. Ion spectra were recorded in the positive mode without fragmentation. A: Free sterols from *Arabidopsis* leaves after SPE purification and derivatization as betainylchloride esters. Cholestanol and stigmastanol were used as internal standards. B: Sterol esters from *Arabidopsis* leaves after two-step SPE purification. The following internal standards were included: 16:0-cholesterol, 16:1-cholesterol, 18:0-cholesterol, and 18:1-cholesterol. C: Sterol glucosides (soybean); internal standards were cholestanol-Glc and stigmastanol-Glc. D: Acylated sterol glucosides (soybean); 16:0-Glc-stigmastanol, 18:0-Glc-stigmastanol, 16:0-Glc-campestanol, and 18:0-Glc-campestanol were the internal standards.

(HPLC chip/MS 1200 with infusion chip; Agilent). Sterol lipids were supplied to the mass spectrometer in methanol-chloroform-300 mM ammonium acetate (665:300:35) (26) at a flow rate of 1 μl min^{-1}. The temperature of the nitrogen gas in the collision cell was 300°C at a flow rate of 8 liters min^{-1}. The fragmentor voltage was 200 V, and the capillary voltage (Vcap) was set to 1,700 V. MS spectra without fragmentation ("MS only" mode) were recorded after every fifth MS/MS spectrum. For MS/MS measurements, the quadrupole was operated in the narrow range (*m/z*, 1.2) and was set at the exact mass of the sterol lipid. Q-TOF MS/MS spectra were accumulated for 1 s, and the signal intensities of at least five different spectra derived from the same parental ion were averaged. Collision energies for MS/MS spectra for betainylated FS, SE, SG, and ASG were 35 V, 13 V, 10 V, and 15 V, respectively.

Data analysis

All sterol lipid classes were quantified by targeted Q-TOF MS/MS analysis. Data were processed using Agilent MassHunter qualitative analysis software. A window of 100 ppm was set for fragment identification. Data obtained by Agilent MassHunter qualitative analysis software were further processed using Microsoft Excel 2007. Free sterols were quantified using the peak size of the betainyl fragment, F_B, of the extracted ion chromatogram function, which corresponds to the precursor ion scan function of a triple quadrupole instrument (see Fig. 3). Betainyl derivatives of unsaturated sterols consistently resulted in lower MS/MS signal intensities than derivatives of saturated sterols. For this reason, a mixture of soybean sterols (campesterol, stigmasterol, and sitosterol), cholestanol, and stigmastanol was quantified by GC

TABLE 1. Profiling of free sterols from *Arabidopsis*

Compound number	Sterol lipid[a]	Formula (M)[b]	(M + betainyl)$^+$ (*m/z*)[c]	Product ion F_B(*m/z*)
1	Cholesterol	$C_{27}H_{46}O$	486.4311	118.0859
2 (I.S.)	Cholestanol	$C_{27}H_{48}O$	488.4468	118.0859
3	Campesterol	$C_{28}H_{48}O$	500.4468	118.0859
4	Stigmasterol	$C_{29}H_{48}O$	512.4468	118.0859
5	Sitosterol	$C_{29}H_{50}O$	514.4624	118.0859
6 (I.S.)	Stigmastanol	$C_{29}H_{52}O$	516.4781	118.0859

I.S., internal standard.

[a] Stigmasterol and isofucosterol were not distinguished by Q-TOF measurements.

[b] Formula of the parental, non-charged molecule.

[c] Molecular weight of the cation formed of the parental molecule after derivatization with *N*-chlorobetainyl chloride.

TABLE 2. Profiling of sterol esters from *Arabidopsis*

Compound number	Sterol ester molecular species[a]	Formula (M)[b]	$(M + NH_4)^+$ (*m/z*)[c]	Product ion F_S (*m/z*)
7	16:3-Cholesterol	$C_{43}H_{70}O_2$	636.5714	369.3505
8	16:2-Cholesterol	$C_{43}H_{72}O_2$	638.5871	369.3505
9 (I.S.)	16:1-Cholesterol	$C_{43}H_{74}O_2$	640.6027	369.3505
10 (I.S.)	16:0-Cholesterol	$C_{43}H_{76}O_2$	642.6184	369.3505
11	16:3-Campesterol	$C_{44}H_{72}O_2$	650.5871	383.3662
12	16:2-Campesterol	$C_{44}H_{74}O_2$	652.6027	383.3662
13	16:1-Campesterol	$C_{44}H_{76}O_2$	654.6184	383.3662
14	16:0-Campesterol	$C_{44}H_{78}O_2$	656.6340	383.3662
15	16:3-Stigmasterol	$C_{45}H_{72}O_2$	662.5871	395.3662
16	16:2-Stigmasterol	$C_{45}H_{74}O_2$	664.6027	395.3662
17	16:3-Sitosterol	$C_{45}H_{74}O_2$	664.6027	397.3818
18	18:3-Cholesterol	$C_{45}H_{74}O_2$	664.6027	369.3505
19	16:1-Stigmasterol	$C_{45}H_{76}O_2$	666.6184	395.3662
20	16:2-Sitosterol	$C_{45}H_{76}O_2$	666.6184	397.3818
21	18:2-Cholesterol	$C_{45}H_{76}O_2$	666.6184	369.3505
22	16:0-Stigmasterol	$C_{45}H_{78}O_2$	668.6340	395.3662
23	16:1-Sitosterol	$C_{45}H_{78}O_2$	668.6340	397.3818
24 (I.S.)	18:1-Cholesterol	$C_{45}H_{78}O_2$	668.6340	369.3505
25	16:0-Sitosterol	$C_{45}H_{80}O_2$	670.6497	397.3818
26 (I.S.)	18:0-Cholesterol	$C_{45}H_{80}O_2$	670.6497	369.3505
27	18:3-Campesterol	$C_{46}H_{76}O_2$	678.6184	383.3662
28	18:2-Campesterol	$C_{46}H_{78}O_2$	680.6340	383.3662
29	18:1-Campesterol	$C_{46}H_{80}O_2$	682.6497	383.3662
30	18:0-Campesterol	$C_{46}H_{82}O_2$	684.6653	383.3662
31	18:3-Stigmasterol	$C_{47}H_{76}O_2$	690.6184	395.3662
32	18:3-Sitosterol	$C_{47}H_{78}O_2$	692.6340	397.3818
33	18:2-Stigmasterol	$C_{47}H_{78}O_2$	692.6340	395.3662
34	20:3-Cholesterol	$C_{47}H_{78}O_2$	692.6340	369.3505
35	18:2-Sitosterol	$C_{47}H_{80}O_2$	694.6497	397.3818
36	18:1-Stigmasterol	$C_{47}H_{80}O_2$	694.6497	395.3662
37	20:2-Cholesterol	$C_{47}H_{80}O_2$	694.6497	369.3505
38	18:0-Stigmasterol	$C_{47}H_{82}O_2$	696.6653	395.3662
39	18:1-Sitosterol	$C_{47}H_{82}O_2$	696.6653	397.3818
40	20:1-Cholesterol	$C_{47}H_{82}O_2$	696.6653	369.3505
41	18:0-Sitosterol	$C_{47}H_{84}O_2$	698.6810	397.3818
42	20:0-Cholesterol	$C_{47}H_{84}O_2$	698.6810	369.3505
43	20:3-Campesterol	$C_{48}H_{80}O_2$	706.6497	383.3662
44	20:2-Campesterol	$C_{48}H_{82}O_2$	708.6653	383.3662
45	20:1-Campesterol	$C_{48}H_{84}O_2$	710.6810	383.3662
46	20:0-Campesterol	$C_{48}H_{86}O_2$	712.6966	383.3662
47	20:3-Stigmasterol	$C_{49}H_{80}O_2$	718.6497	395.3662
48	22:3-Cholesterol	$C_{49}H_{82}O_2$	720.5245	369.3505
49	20:2-Stigmasterol	$C_{49}H_{82}O_2$	720.6653	395.3662
50	20:3-Sitosterol	$C_{49}H_{82}O_2$	720.6653	397.3818
51	20:1-Stigmasterol	$C_{49}H_{84}O_2$	722.6810	395.3662
52	20:2-Sitosterol	$C_{49}H_{84}O_2$	722.6810	397.3818
53	22:2-Cholesterol	$C_{49}H_{84}O_2$	722.6810	369.3505
54	20:0-Stigmasterol	$C_{49}H_{86}O_2$	724.6966	395.3662
55	20:1-Sitosterol	$C_{49}H_{86}O_2$	724.6966	397.3818
56	22:1-Cholesterol	$C_{49}H_{86}O_2$	724.6966	369.3505
57	20:0-Sitosterol	$C_{49}H_{88}O_2$	726.7123	397.3818
58	22:0-Cholesterol	$C_{49}H_{88}O_2$	726.7123	369.3505
59	22:3-Campesterol	$C_{50}H_{84}O_2$	734.5401	383.3662
60	22:2-Campesterol	$C_{50}H_{86}O_2$	736.6966	383.3662
61	22:1-Campesterol	$C_{50}H_{88}O_2$	738.7123	383.3662
62	22:0-Campesterol	$C_{50}H_{90}O_2$	740.7279	383.3662
63	22:3-Stigmasterol	$C_{51}H_{84}O_2$	746.5401	395.3662
64	22:3-Sitosterol	$C_{51}H_{86}O_2$	748.5558	397.3818
65	22:2-Stigmasterol	$C_{51}H_{86}O_2$	748.6966	395.3662
66	22:1-Stigmasterol	$C_{51}H_{88}O_2$	750.7123	395.3662
67	22:2-Sitosterol	$C_{51}H_{88}O_2$	750.7123	397.3818
68	22:0-Stigmasterol	$C_{51}H_{90}O_2$	752.7279	395.3662
69	22:1-Sitosterol	$C_{51}H_{90}O_2$	752.7279	397.3818
70	22:0-Sitosterol	$C_{51}H_{92}O_2$	754.7436	397.3818

I.S., internal standard.

[a] Stigmasterol and isofucosterol were not distinguished by Q-TOF measurements.

[b] Formula of the parental, non-charged molecule.

[c] Molecular weight of the cation formed of the parental molecule with ammonium.

and by Q-TOF MS/MS. From this experiment, a correction factor for unsaturated sterols was calculated (1.61 ± 0.06; $n = 7$). SEs were quantified by the formation of sterol-specific fragments (F_S) (Fig. 1). Two pairs of internal standards were used to compensate for the differences in ion suppression for SEs with saturated or unsaturated acyl groups (**Fig. 2**). SGs show different fragmentation patterns depending on their degree of unsaturation of the sterol moiety (see Fig. 4). Therefore, a mixture of unsaturated and saturated SGs was measured via GC and Q-TOF MS/MS. After normalization to the same molar quantity, the Q-TOF MS/MS F_S peak intensity was found to be reproducibly smaller for saturated SG than for unsaturated SG by a factor of 0.169 ± 0.017 ($n = 3$). This factor was used for the correction during Q-TOF MS/MS measurements of unsaturated SGs. ASGs with an unsaturated sterol moiety showed a different fragmentation pattern with a high F_S peak, while ASGs with a saturated sterol group showed a high acyl-glucoside-specific fragment (F_{AG}) (see Fig. 4). Quantification of the F_S and F_{AG} fragment peaks in a mixture of soybean ASGs (containing mostly unsaturated sterols) and hydrogenated ASGs (containing saturated sterols) by Q-TOF MS/MS revealed that the signal responses for ASGs with unsaturated and saturated sterol moieties were comparable, and, therefore, no correction factor was required. Exact masses of all molecular sterol species and isotopic distribution of the MS/MS fragments derived from the presence of ^{13}C isotopes were calculated using the Agilent MassHunter mass calculator and the Isotope Distribution Calculator tools. Targeted lists for the molecular species of all sterol classes are displayed in **Tables 1–4**. Isotopic correction was applied in all cases where a molecular species exists that contains one additional double bond (i.e., *m/z* M-2) in the sterol moiety or in the acyl chain, as outlined in a previous study (45). A linear regression line was calculated for the two pairs of standards used for each lipid class to account for the dependence of ionization on the size (*m/z*) of the parental ion (46). The contents of molecular species were calculated in μmol g^{-1} FW.

RESULTS

Measurement of sterol lipids by Q-TOF MS/MS

Direct infusion MS/MS experiments using a triple-quadrupole or a Q-TOF mass spectrometer represent a robust and reliable method for the identification and quantification of complex lipids (26, 28, 46, 47). This strategy has been successfully applied to the measurements of phosphoglycerolipids, glycoglycerolipids, sphingolipids, and triacylglycerols in plants, animals, and yeast (28). A major drawback of this approach can originate from differences in the ionization efficiency of molecules from a complex matrix. It is well known that the polarity of a molecule is a major determinant for the ionization efficiency in the ion source. Therefore, nonpolar molecules can suffer from severe ion suppression during ionization. The four sterol lipid classes present in plants strongly differ in their polarities, with FS and SE representing nonpolar lipids, while SG and ASG are polar lipids. To study the influence of ion suppression, a dilution series was generated from a crude *Arabidopsis* leaf lipid extract, and peak signals for sterol lipids were observed in the MS and MS/MS modes of the nanospray Q-TOF mass spectrometer. Strong ion suppression was observed for FS and SE, while SG and ASG were less affected (data not shown). Therefore, the lipid extract

TABLE 3. Profiling of sterol glucosides from *Arabidopsis*

Compound number	Sterol glucoside molecular species[a]	Formula (M)[b]	$(M+NH_4)^+$ (*m/z*)[c]	Product ion F_S (*m/z*)
71	Glc-Cholesterol	$C_{33}H_{56}O_6$	566.4415	369.3505
72 (I.S.)	Glc-Cholestanol	$C_{33}H_{58}O_6$	568.4572	371.3662
73	Glc-Campesterol	$C_{34}H_{58}O_6$	580.4572	383.3662
74	Glc-Stigmasterol	$C_{35}H_{58}O_6$	592.4572	395.3662
75	Glc-Sitosterol	$C_{35}H_{60}O_6$	594.4728	397.3818
76 (I.S.)	Glc-Stigmastanol	$C_{35}H_{62}O_6$	596.4885	399.3975

I.S., internal standard.
[a] Stigmasterol and isofucosterol were not distinguished by Q-TOF measurements.
[b] Formula of the parental, non-charged molecule.
[c] Molecular weight of the cation formed of the parental molecule with ammonium.

was fractionated via SPE on silica columns, and two fractions containing nonpolar lipids (FS and SE) or polar lipids (SG and ASG) were harvested (Fig. 1). This additional purification step resulted in a strong improvement of ionization efficiency for all sterol lipid classes, in particular for nonpolar sterol lipids, and was therefore employed for all further analyses.

Infusion of lipids in methanol-chloroform containing aqueous ammonium acetate resulted in the ionization of most sterol lipids (SE, SG, and ASG) as ammonium adducts (Fig. 2). Free sterols, however, were poorly ionized, and, upon fragmentation, many small fragments were produced, whose number and size depended on the structure of the respective sterol. Derivatization of target molecules has been shown to improve ionization and, furthermore, during fragmentation can yield a strong leaving group, which can be selected in a precursor ion or neutral loss scanning experiment. Free cholesterol, dehydrocholesterol, and oxysterols were previously quantified in MS/MS experiments after derivatization to esters of mono-(dimethylaminoethyl)-succinate, *N,N*-dimethylglycine, picolinate, or acetate or to hydrazones (30–33). Derivatization of FSs from yeast with acetylchloride resulted in the synthesis of sterol acetates that were detected as sterol ions after fragmentation (28). Acetylation of FSs from *Arabidopsis* leaves resulted in high background signals (data not shown). Derivatization with *N*-chlorobetainyl chloride has previously been shown to improve ionization of diacylglycerol in MS/MS experiments (43). Therefore, FSs from *Arabidopsis* leaves were betainylated with *N*-chlorobetainyl chloride, thereby adding a permanent positive charge to the molecule. Betainylated sterols were easily ionized without further adduct formation and yielded a characteristic cation fragment for the betainyl group after collision induced fragmentation (**Fig. 3**).

Sterol quantification with internal standards

For each lipid class, at least two internal standards were used for quantification to correct for the differences in signal intensity, which has been shown to be dependent on the mass of the parental ion (26, 46). Saturated sterols are absent from plants and can therefore serve as suitable internal standards. Thus, cholestanol and stigmastanol were used as internal standards for free sterol measurements. Because of their low polarity, SEs are susceptible to ion suppression, in particular SEs carrying a saturated fatty acid residue, while SEs with unsaturated fatty acids are less affected. Previously, liquid chromatography MS analysis with a quadrupole ion trap instrument revealed that signal intensities of SEs were increased depending on the degree of saturation of the acyl group (48). Direct infusion nanospray MS/MS with a Q-TOF instrument showed that the signal intensities for SEs carrying mono-, di-, and triunsaturated acyl groups were comparable. To compensate for partial ion suppression of SEs with saturated acyl groups, two pairs of internal standards were added. The pairs of 16:0-cholesterol/18:0-cholesterol and 16:1-cholesterol/18:1-cholesterol were employed for the measurement of SEs with saturated and unsaturated fatty acids, respectively. For the quantification of SGs, cholestanol-Glc and stigmastanol-Glc were chemically synthesized. For ASGs, a commercially available ASG fraction from soybean was hydrogenated. Two fully saturated ASGs, 16:0-Glc-stigmastanol and 18:0-Glc-stigmastanol, were then used as internal standards for ASG quantification.

Fragmentation patterns of sterol lipids

The basis for lipid quantification via direct infusion MS/MS is the selection of the parental ion in the first quadrupole, the fragmentation in the collision cell, and the identification and quantification of a characteristic fragment peak in the last quadrupole (for triple-quadrupole mass spectrometers) or in the TOF mass analyzer (for Q-TOF). The fragmentor voltage was optimized to avoid premature fragmentation of conjugated sterols before reaching the collision cell. Furthermore, collision energies were optimized for maximal signal intensities for the desired fragments. The selected fragment ions are shown in **Figs.** 3 and **4**.

Betainylated FSs carry a permanent positive charge that renders adduct formation unnecessary. Fragmentation resulted in the neutral loss of the sterol backbone (Fig. 3, shown as N_S) and in the detection of the characteristic betainyl cation at *m/z* of 118.0859. Fragmentation of ammonium adducts of SEs led to the neutral loss of the respective acyl groups (Fig. 3). The signal of the sterol-specific backbone fragment (F_S) was used for quantification.

Similarly, fragmentation of SG produced an F_S peak corresponding to that of the sterol backbone (Fig. 4). Comparison of signal intensities obtained in the MS mode with those obtained in the MS/MS mode confirmed that fragmentation of unsaturated SGs yields a high peak for the F_S

TABLE 4. Profiling of acylated sterol glucosides from *Arabidopsis*

Compound number	Acylated sterol glucoside molecular species[a]	Formula (M)[b]	$(M+NH_4)^+$ (*m/z*)[c]	Product ion F_S (*m/z*)	Product ion F_{AG} (*m/z*)
77	16:3-Glc-Cholesterol	$C_{49}H_{80}O_7$	798.6242	369.3505	395.2428
78	16:2 Glc-Cholesterol	$C_{49}H_{82}O_7$	800.6399	369.3505	397.2585
79	16:1-Glc-Cholesterol	$C_{49}H_{84}O_7$	802.6555	369.3505	399.2741
80	16:0-Glc-Cholesterol	$C_{49}H_{86}O_7$	804.6712	369.3505	401.2898
81	16:3-Glc-Campesterol	$C_{50}H_{82}O_7$	812.6399	383.3662	395.2428
82	16:2-Glc-Campesterol	$C_{50}H_{84}O_7$	814.6555	383.3662	397.2585
83	16:1-Glc-Campesterol	$C_{50}H_{86}O_7$	816.6712	383.3662	399.2741
84	16:0-Glc-Campesterol	$C_{50}H_{88}O_7$	818.6868	383.3662	401.2898
85 (I.S.)	16:0-Glc-Campestanol	$C_{50}H_{90}O_7$	820.7025	385.3818	401.2898
86	16:3-Glc-Stigmasterol	$C_{51}H_{82}O_7$	824.6399	395.3662	395.2428
87	16:2-Glc-Stigmasterol	$C_{51}H_{84}O_7$	826.6555	395.3662	397.2585
88	16:3-Glc-Sitosterol	$C_{51}H_{84}O_7$	826.6555	397.3818	395.2428
89	18:3-Glc-Cholesterol	$C_{51}H_{84}O_7$	826.6555	369.3505	423.2741
90	16:1-Glc-Stigmasterol	$C_{51}H_{86}O_7$	828.6712	395.3662	399.2741
91	16:2-Glc-Sitosterol	$C_{51}H_{86}O_7$	828.6712	397.3818	397.2585
92	18:2 Glc-Cholesterol	$C_{51}H_{86}O_7$	828.6712	369.3505	425.2898
93	16:0-Glc-Stigmasterol	$C_{51}H_{88}O_7$	830.6868	395.3662	401.2898
94	16:1-Glc-Sitosterol	$C_{51}H_{88}O_7$	830.6868	397.3818	399.2741
95	18:1-Glc-Cholesterol	$C_{51}H_{88}O_7$	830.6868	369.3505	427.3054
96	16:0-Glc-Sitosterol	$C_{51}H_{90}O_7$	832.7025	397.3818	401.2898
97	18:0-Glc-Cholesterol	$C_{51}H_{90}O_7$	832.7025	369.3505	429.3211
98 (I.S.)	16:0-Glc-Stigmastanol	$C_{51}H_{92}O_7$	834.7181	399.3975	401.2898
99	18:3-Glc-Campesterol	$C_{52}H_{86}O_7$	840.6712	383.3662	423.2741
100	18:2-Glc-Campesterol	$C_52H_{88}O_7$	842.6868	383.3662	425.2898
101	18:1-Glc-Campesterol	$C_{52}H_{90}O_7$	844.7025	383.3662	427.3054
102	18:0-Glc-Campesterol	$C_{52}H_{92}O_7$	846.7181	383.3662	429.3211
103 (I.S.)	18:0-Glc-Campestanol	$C_{52}H_{94}O_7$	848.7338	385.3818	429.3211
104	18:3-Glc-Stigmasterol	$C_{53}H_{86}O_7$	852.6712	395.3662	423.2741
105	18:3-Glc-Sitosterol	$C_{53}H_{88}O_7$	854.6868	397.3818	423.2741
106	18:2-Glc-Stigmasterol	$C_{53}H_{88}O_7$	854.6868	395.3662	425.2898
107	20:3-Glc-Cholesterol	$C_{53}H_{88}O_7$	854.6868	369.3505	451.3054
108	18:2-Glc-Sitosterol	$C_{53}H_{90}O_7$	856.7025	397.3818	425.2898
109	18:1-Glc-Stigmasterol	$C_{53}H_{90}O_7$	856.7025	395.3662	427.3054
110	20:2-Glc-Cholesterol	$C_{53}H_{90}O_7$	856.7025	369.3505	453.3211
111	18:0-Glc-Stigmasterol	$C_{53}H_{92}O_7$	858.7181	395.3662	429.3211
112	18:1-Glc-Sitosterol	$C_{53}H_{92}O_7$	858.7181	397.3818	427.3054
113	20:1-Glc-Cholesterol	$C_{53}H_{92}O_7$	858.7181	369.3505	455.3367
114	18:0-Glc-Sitosterol	$C_{53}H_{94}O_7$	860.7338	397.3818	429.3211
115	20:0-Glc-Cholesterol	$C_{53}H_{94}O_7$	860.7338	369.3505	457.3524
116 (I.S.)	18:0-Glc-Stigmastanol	$C_{53}H_{96}O_7$	862.7494	399.3975	429.3211
117	20:3-Glc-Campesterol	$C_{54}H_{90}O_7$	868.7025	383.3662	451.3054
118	20:2-Glc-Campesterol	$C_54H_{92}O_7$	870.7181	383.3662	453.3211
119	20:1-Glc-Campesterol	$C_{54}H_{94}O_7$	872.7338	383.3662	455.3367
120	20:0-Glc-Campesterol	$C_{54}H_{96}O_7$	874.7494	383.3662	457.3524
121	20:3-Glc-Stigmasterol	$C_{55}H_{90}O_7$	880.7025	395.3662	451.3054
123	22:3-Glc-Cholesterol	$C_{55}H_{92}O_7$	882.5773	369.3505	479.3367
124	20:2-Glc-Stigmasterol	$C_{55}H_{92}O_7$	882.7181	395.3662	453.3211
125	20:3-Glc-Sitosterol	$C_55H_{92}O_7$	882.7181	397.3818	451.3054
126	20:1-Glc-Stigmasterol	$C_{55}H_{94}O_7$	884.7338	395.3662	455.3367
127	20:2-Glc-Sitosterol	$C_{55}H_{94}O_7$	884.7338	397.3818	453.3211
128	22:2-Glc-Cholesterol	$C_{55}H_{94}O_7$	884.7338	369.3505	481.3524
129	20:0-Glc-Stigmasterol	$C_{55}H_{96}O_7$	886.7494	395.3662	457.3524
130	20:1-Glc-Sitosterol	$C_{55}H_{96}O_7$	886.7494	397.3818	455.3367
131	22:1-Glc-Cholesterol	$C_{55}H_{96}O_7$	886.7494	369.3505	483.3680
132	20:0-Glc-Sitosterol	$C_{55}H_{98}O_7$	888.7651	397.3818	457.3524
133	22:0-Glc-Cholesterol	$C_{55}H_{98}O_7$	888.7651	369.3505	485.3837
134	22:3-Glc-Campesterol	$C_{56}H_{94}O_7$	896.5929	383.3662	479.3367
135	22:2-Glc-Campesterol	$C_{56}H_{96}O_7$	898.7494	383.3662	481.3524
136	22:1-Glc-Campesterol	$C_{56}H_{98}O_7$	900.7651	383.3662	483.3680
137	22:0-Glc-Campesterol	$C_{56}H_{100}O_7$	902.7807	383.3662	485.3837
138 (I.S.)	22:0-Glc-Campestanol	$C_{56}H_{102}O_7$	904.7964	385.3818	485.3837
139	22:3-Glc-Stigmasterol	$C_{57}H_{94}O_7$	908.5929	395.3662	479.3367
140	22:3-Glc-Sitosterol	$C_{57}H_{96}O_7$	910.6086	397.3818	479.3367
141	22:2-Glc-Stigmasterol	$C_{57}H_{96}O_7$	910.7494	395.3662	481.3524
142	22:1-Glc-Stigmasterol	$C_{57}H_{98}O_7$	912.7651	395.3662	483.3680
143	22:2-Glc-Sitosterol	$C_{57}H_{98}O_7$	912.7651	397.3818	481.3524
144	22:0-Glc-Stigmasterol	$C_{57}H_{100}O_7$	914.7807	395.3662	485.3837
145	22:1-Glc-Sitosterol	$C_{57}H_{100}O_7$	914.7807	397.3818	483.3680
146	22:0-Glc-Sitosterol	$C_{57}H_{102}O_7$	916.7964	397.3818	485.3837
147 (I.S.)	22:0-Glc-Stigmastanol	$C_{57}H_{104}O_7$	918.8120	399.3975	485.3837

I.S., internal standard.
[a] Stigmasterol and isofucosterol were not distinguished by Q-TOF measurements.
[b] Formula of the parental, non-charged molecule.
[c] Molecular weight of the cation formed of the parental molecule with ammonium.

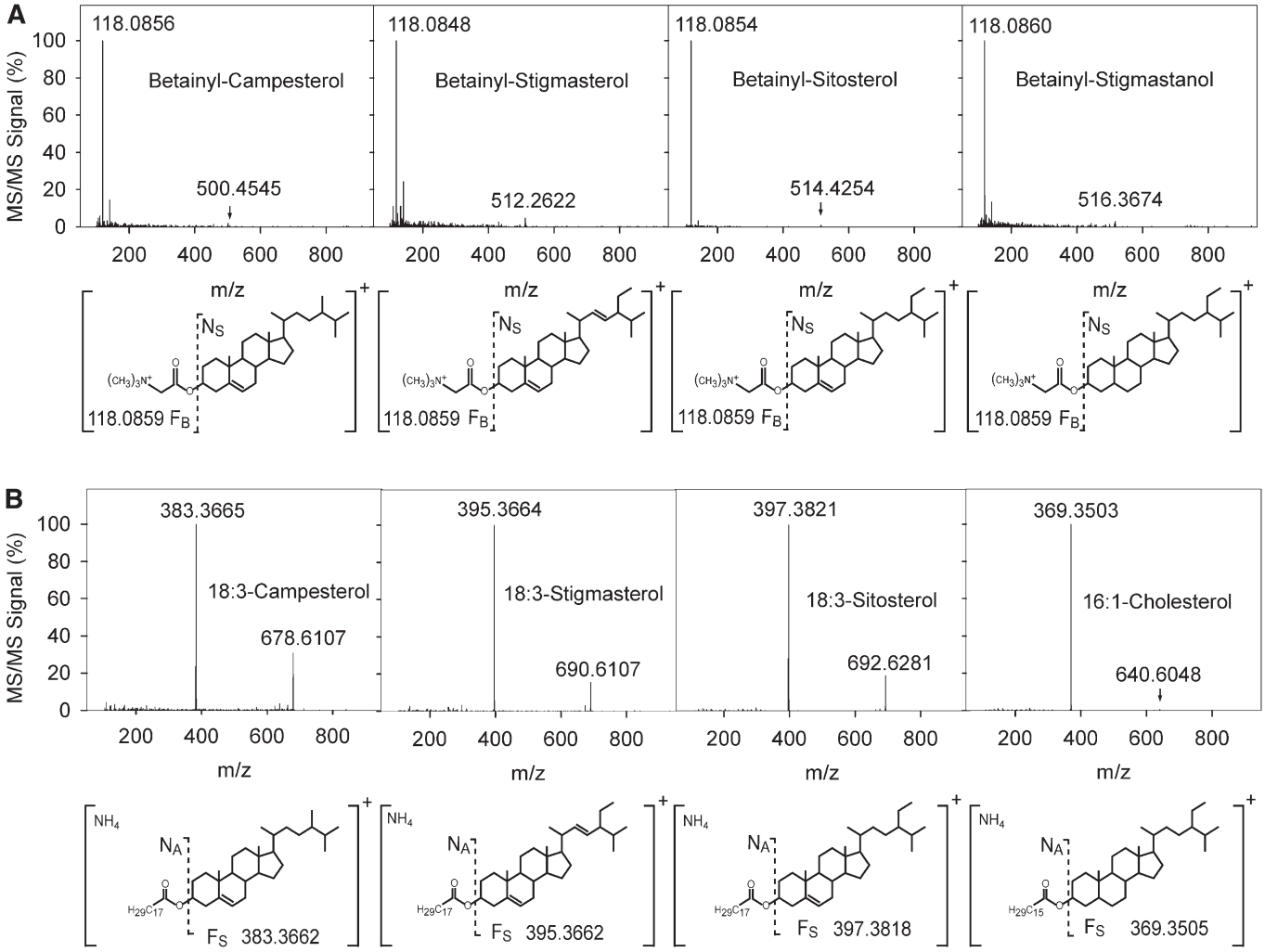

Fig. 3. Fragmentation pattern of free sterols and sterol esters. A: Q-TOF MS/MS spectra of betainylated FSs with the corresponding fragmentation patterns and calculated masses. Fragmentation of the betainyl derivatives of sitosterol, stigmasterol, campesterol, and stigmastanol (internal standard) results in the neutral loss of the sterol moiety along with the accumulation of the betainyl fragment F_B at *m/z* of 118.0859. B: Q-TOF MS/MS spectra of SEs. Fragmentation of the ammonium adducts of SEs leads to the release of the corresponding sterol cation F_S. 16:1-cholesterol was used as the internal standard.

(Fig. 4). For saturated SGs, the F_S peak was much smaller, and a number of additional peaks occurred at lower *m/z*. This was of particular importance because the internal standards contained saturated sterol moieties, while plant SGs contain mostly unsaturated sterols. Application of correction factors has previously been described for the quantification of sphingolipid classes (3). A similar approach was therefore followed for the quantification of SGs by calculation of a correction factor to compensate for the lower F_S signal intensities of saturated versus unsaturated SGs.

Similar to SGs, the fragmentation pattern of the ASGs was different when one or more double bonds were present in the sterol moiety (Fig. 4). The fragmentation of ASGs carrying unsaturated sterol moieties resulted in the accumulation of a large peak for the sterol fragment F_S (Fig. 4). Fragmentation of ASGs with a saturated sterol backbone, however, led to the formation of a large peak for the F_{AG} (Fig. 4). Therefore, the F_S and F_{AG} fragment peaks were employed for quantification of ASGs with unsaturated or saturated sterol moieties, respectively.

The linearity of signal intensities was evaluated for each sterol lipid class, using the corresponding standards. To compensate for fluctuations in the nanospray flow of the ion source, the signal of each sterol lipid standard was normalized to a second internal standard of the same lipid class, which was kept at constant concentration. The standard curves of the normalized, logarithmic signals were then plotted relative to the logarithmic amount of the variable standard (**Fig. 5**). Standard curves showed that the signals were linear over a range of 3 to 4 orders of magnitude for FS, SE, and SG and greater than 2 orders of magnitude for ASG. Correlation coefficients for linearity for all four lipid classes were calculated to be higher than 0.99.

Scanning for molecular species composition of sterol lipids in *Arabidopsis* leaves

Sitosterol and campesterol were previously shown to be the most abundant sterols in *Arabidopsis* (15, 49). Cholesterol, stigmasterol, and isofucosterol are minor

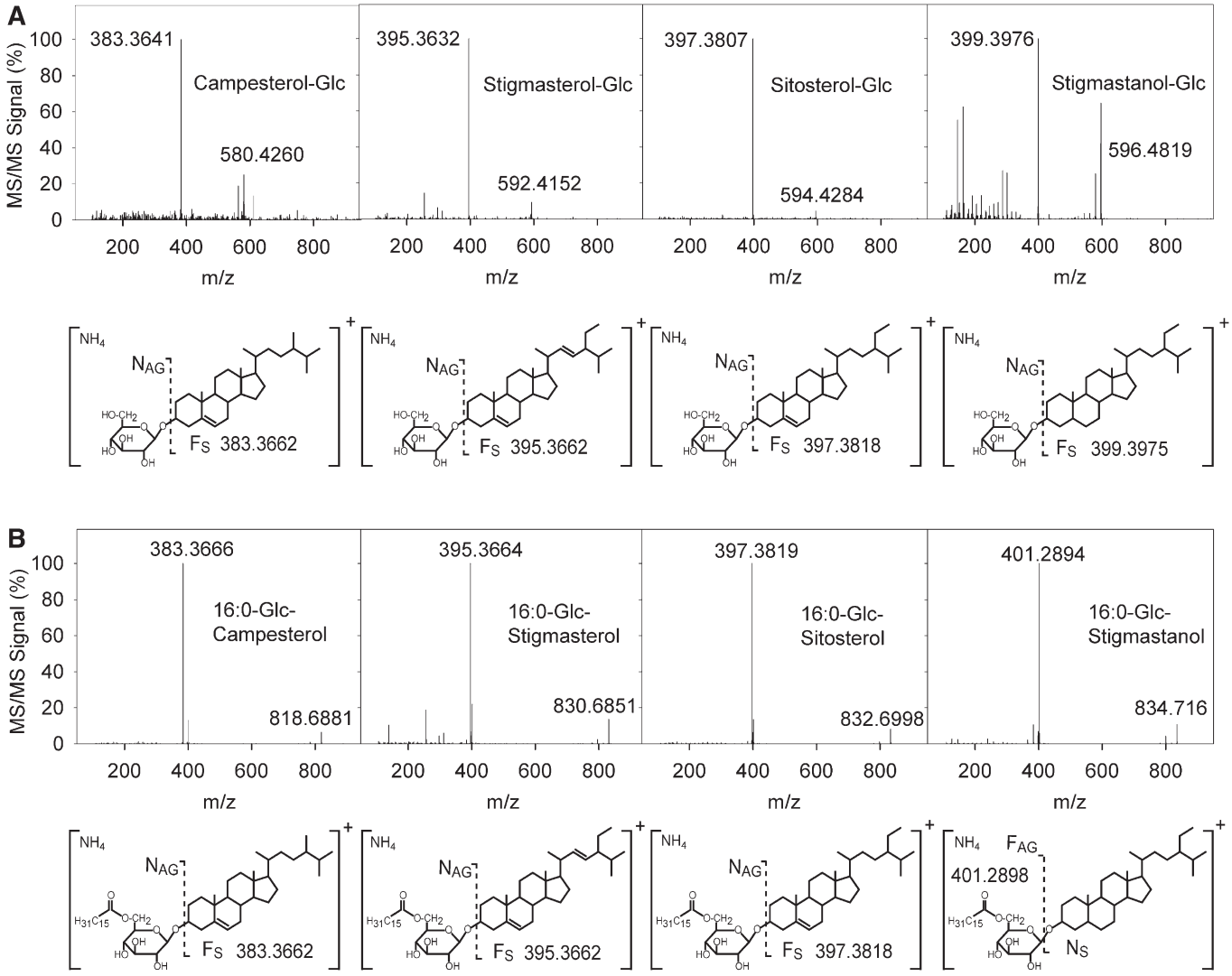

Fig. 4. Fragmentation pattern of sterol glucosides and acylated sterol glucosides. A: Q-TOF MS/MS spectra of different SGs. Collision induced dissociation of the ammonium adduct of SGs produces a sterol fragment F_S. The spectrum of the saturated stigmastanol-Glc (used as the internal standard) reveals a peak of lower intensity corresponding to the sterol fragment F_s and the presence of additional peaks. B: Q-TOF MS/MS spectra of ASGs. Note that fragmentation of ASGs with unsaturated sterol moieties leads to the release of the sterol cation F_S. Fragmentation of ASGs with saturated sterol moieties (16:0-Glc-stigmastanol, internal standard) leads to the accumulation of a peak at 401.2898, corresponding to the 16:0-Glc cation.

components. Nontargeted screening for molecular species of sterol lipids using the Q-TOF MS and MS/MS modes confirmed this result (data not shown). Therefore, these sterols were selected for a targeted approach to quantify the different sterol lipid classes. As stigmasterol and isofucosterol are isomeric and, therefore, conjugated sterol lipids containing either of these two sterols yield isobaric fragments after collision induced dissociation, they were quantified together. For SE and ASG, a large number of molecular species carrying different acyl groups were detected by MS and MS/MS experiments, with acyl groups ranging from 16 to 22 carbon atoms and containing 0 to 3 double bonds. While not all of these acyl groups were found in SEs or ASGs of *Arabidopsis*, a wide range of molecular species was selected for targeted MS/MS analysis to cover possible alterations in the fatty acid pattern during stress or in different plant species (**Fig. 6**). The most abundant SEs in *Arabidopsis* leaves were 18:3-sitosterol and 18:2-sitosterol. Interestingly, a considerable amount of SEs contained very-long-chain fatty acids, e.g., 20:0-cholesterol and 20:0-sitosterol. The molecular species pattern of ASGs was dominated by 16:0-Glc-sitosterol, with smaller amounts of 18:3-Glc-sitosterol and 18:2-Glc-sitosterol (Fig. 6). Targeted lists including the masses of all sterol lipid classes for parental ions and the fragment ions used for quantification are displayed in Tables 1–4.

Comparison of sterol lipid quantification by Q-TOF MS/MS and TLC/GC

TLC/GC quantification of sterol lipids from *Arabidopsis* leaves was used to validate the quantification results acquired by Q-TOF MS/MS. To this end, a total lipid extract from *Arabidopsis* leaves including internal standards was

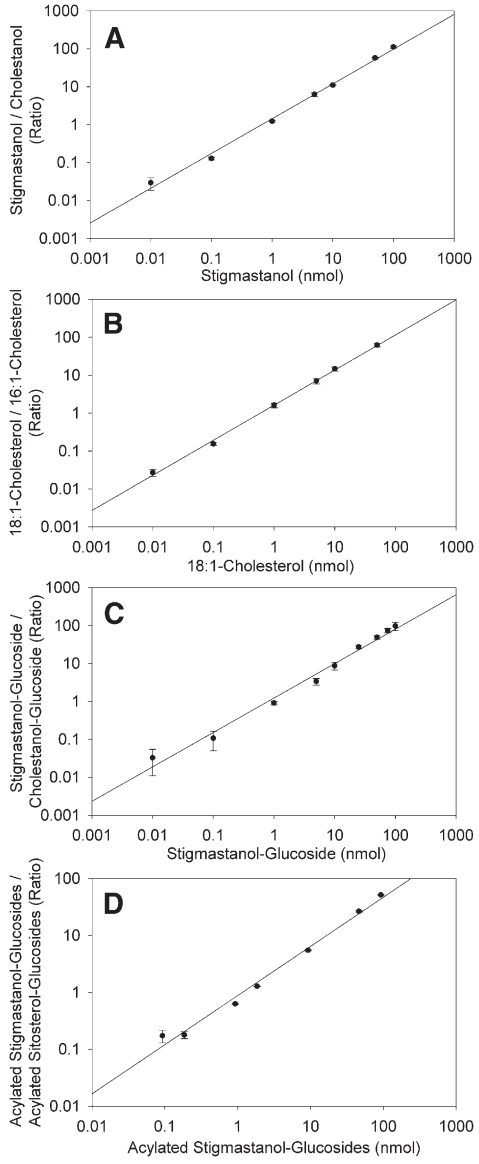

Fig. 5. Standard curves for sterol lipids. Different amounts of each lipid standard were infused into the Q-TOF mass spectrometer in the presence of a constant amount of an internal standard, and the ratio of the MS/MS signals was plotted against the variable standard content (in nmol per 200 µl). The data show the means ± SD of at least three experiments and regression lines. Axes show logarithmic scaling. A: Standard curve for stigmastanol normalized to cholestanol. B: Standard curve for 18:1-cholesterol normalized to 16:1-cholesterol. C: Standard curve for stigmastanol-Glc normalized to cholestanol-Glc. D: Standard curve for acylated stigmastanol-glucoside normalized to acylated sitosterol-glucoside.

fractionated into nonpolar (FS and SE) and polar (SG and ASG) sterols via SPE on silica columns. One aliquot was taken for Q-TOF analysis. A second aliquot was used for further separation by SPE and TLC and quantification by GC after hydrolysis and silylation (Fig. 1). **Figure 7** shows a comparison of the sterol lipid contents as measured by TLC/GC and Q-TOF MS/MS. The two methods resulted in the same overall composition and comparable absolute amounts of sterol lipids from *Arabidopsis* leaves. FSs represent the predominant sterol lipid class, while SEs and SGs are less abundant, and ASGs represent a minor lipid class.

Changes in sterol lipid composition during phosphate deprivation

Phosphate deficiency represents one of the most severe stimuli for alterations of membrane lipid composition in plants. While the changes in the contents of phosphoglycerolipids and glycoglycerolipids during phosphate deficiency have been well documented, the effects on the amounts of sterol lipids are less clear. Therefore, the content and composition of sterol lipids were measured by Q-TOF MS/MS after phosphate deprivation. Lipids were isolated from leaves or roots of *Arabidopsis* plants grown on synthetic medium with or without phosphate. Furthermore, lipids were extracted from the *Arabidopsis pho1* mutant. Leaves of the *pho1* mutant are phosphate-deficient due to a mutation in a phosphate transporter that affects phosphate transport from the root to the shoot (38, 50). **Figure 8** shows the sterol lipid content measured by Q-TOF MS/MS in leaves of the wild type (WT) and the *pho1* mutant and in leaves and roots of plants grown on synthetic medium in the presence or absence of phosphate. Phosphate deprivation caused a significant ($P < 0.02$) increase in the amounts of SG and ASG in leaves, which could also be detected in leaves of the *pho1* mutant, compared with those in the WT. The amount of SG was also significantly increased in roots during phosphate deprivation, while the ASG content in roots was not affected. At the same time, the content of FS was slightly increased in leaves of phosphate-deprived plants, but this change was not significant, and FS remained unchanged in roots. These findings were in accordance with data previously obtained from phosphate-limited oat (22). The amounts of SE were significantly increased in phosphate-deprived leaves and phosphate-deprived roots of the *pho1* mutant. Furthermore, leaves of *Arabidopsis* plants grown on synthetic medium consistently contained a higher SE content than soil-grown plants, which was further increased during phosphate deprivation (Fig. 8).

The amounts of cholesterol, campesterol, stigmasterol/isofucosterol, and sitosterol in the different sterol lipid classes were very similar upon phosphate deprivation (**Fig. 9**). Although some of the changes were calculated to be significant ($P < 0.02$), the differences were minor. **Figure 10** shows alterations in fatty acid composition of SEs and ASGs during phosphate deprivation. The 18:2 content of SEs in the *pho1* mutant and in the leaves of WT plants grown in the absence of phosphate was significantly reduced ($P < 0.02$). At the same time, the amounts of 18:3 content in SEs were significantly increased. Furthermore, a substantial proportion of saturated very-long-chain (20:0; 22:0) acyl groups were found in SEs of WT roots, and the amounts of these acyl groups were significantly decreased during phosphate deprivation. In leaves, the amounts of 18:2 ASGs were significantly decreased during phosphate deprivation with a concomitant increase in 18:3, similar to the changes in

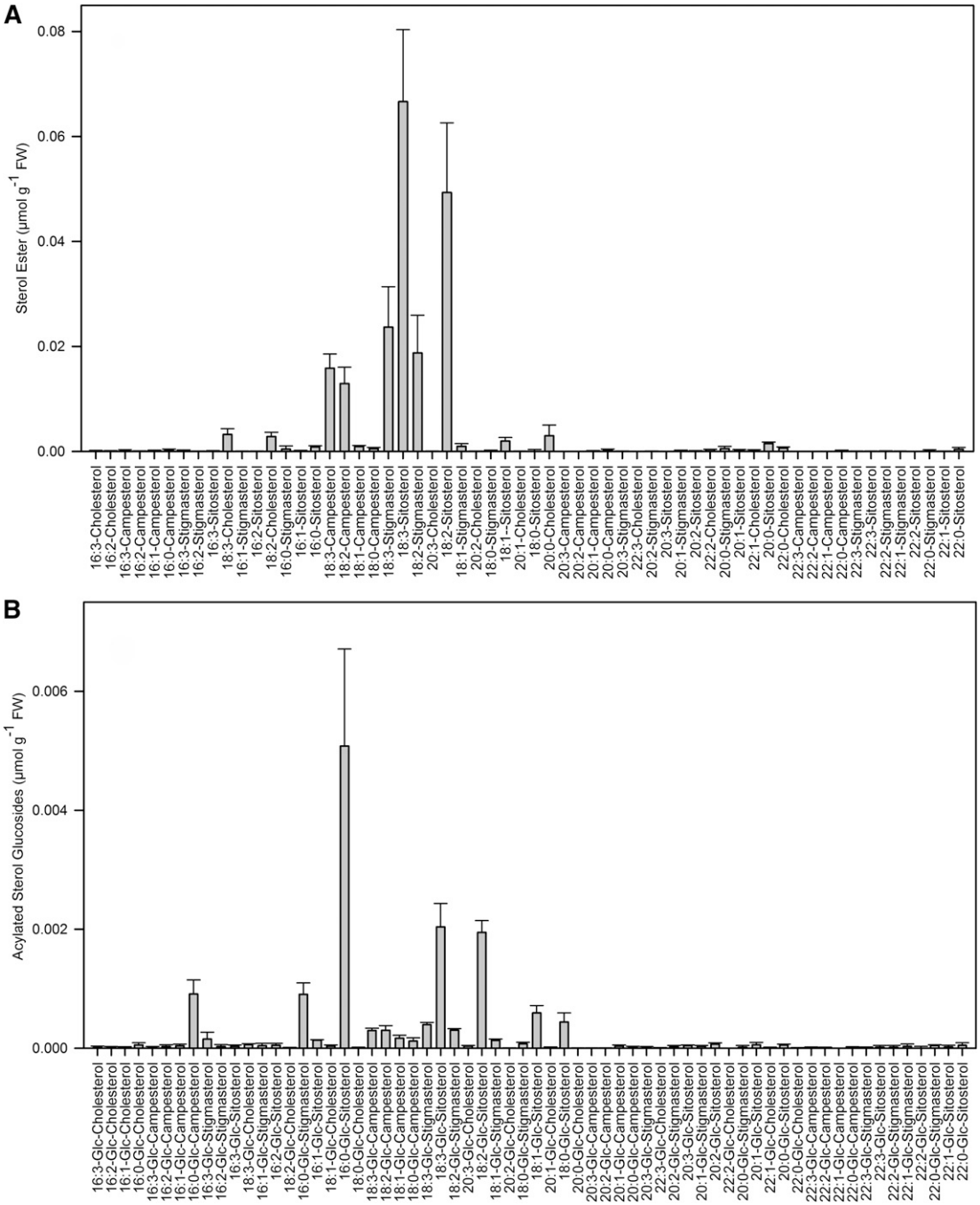

Fig. 6. Molecular species composition of sterol esters and acylated sterol glucosides determined by Q-TOF MS/MS. A: Sterol esters; (B) acylated sterol glucosides. Data show means ± SD of four measurements. Stigmasterol and isofucosterol-containing molecular species were not distinguished as these two sterols are isomeric.

acyl composition of SEs. In roots, 16:0 was significantly decreased in ASGs with a concomitant accumulation of 18:3, indicating that there was a shift from saturated to unsaturated acyl groups.

DISCUSSION

The development of high-resolution mass spectrometers has provided the means for the establishment of new approaches to the identification and quantification of plant metabolites. In contrast to GC-based methods, which usually depend on hydrolyzation and derivatization of complex lipids, nondestructive methods are required for the direct measurements of membrane and storage lipids. Here we describe the development of a comprehensive strategy for the identification and quantification of the molecular species of all known sterol lipid classes in plants via Q-TOF MS/MS.

Sterol lipid classes in plants differ with regard to their polarity, which determines the ionization and fragmentation characteristics in MS and MS/MS experiments. Attempts to measure the molecular species of all four sterol

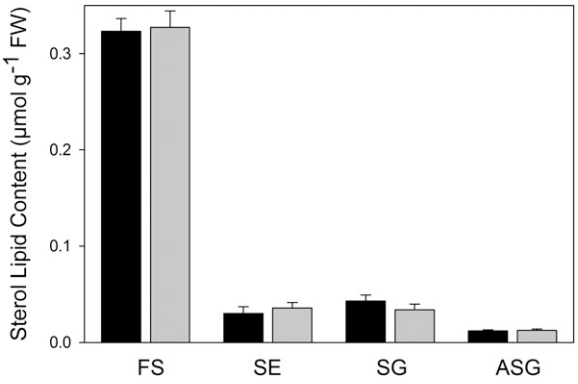

Fig. 7. Comparison of sterol lipid quantification by Q-TOF MS/MS measurements versus those with TLC/GC. Lipids were isolated from *Arabidopsis* leaves in the presence of internal standards and fractionated by SPE into nonpolar lipids (FS, SE) and polar lipids (SG, ASG). One aliquot each was analyzed by TLC/GC (black bars) or by Q-TOF MS/MS (gray bars). Bars show means ± SD of four measurements.

lipid classes by direct infusion MS/MS experiments of a crude lipid extract were not satisfactory. The ionization efficiency of the different sterol lipids was strongly improved after SPE on silica columns. However, ionization efficiency of FSs was still inadequate. Conversion of FS into betainyl derivatives strongly improved ionization and provided the means for detection of a strong leaving group in MS/MS. Ionization of SEs was dependent on the presence or absence of a double bond in the acyl chain. SEs with saturated acyl chains were more prone to ion suppression than those containing at least one double bond. For this reason, the saturated and unsaturated SEs were quantified relative to the respective saturated or unsaturated internal SE standards.

While ionization efficiency of SGs and ASGs was high, their fragmentation patterns were found to depend

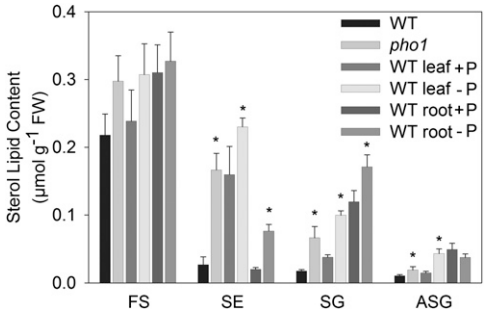

Fig. 8. Sterol lipid content in *Arabidopsis* leaves and roots during phosphate deprivation measured by Q-TOF MS/MS. Lipids were extracted from *Arabidopsis* leaves of WT and *pho1* mutant plants grown on soil and from leaves and roots of WT plants grown on synthetic medium with or without phosphate. The bars show sterol lipid content (means ± SD of five measurements). Data were confirmed by a second independent biological experiment. Values significantly different from those of the WT or from the phosphate-containing control are indicated by an asterisk (according to Student's *t* test; $P < 0.02$).

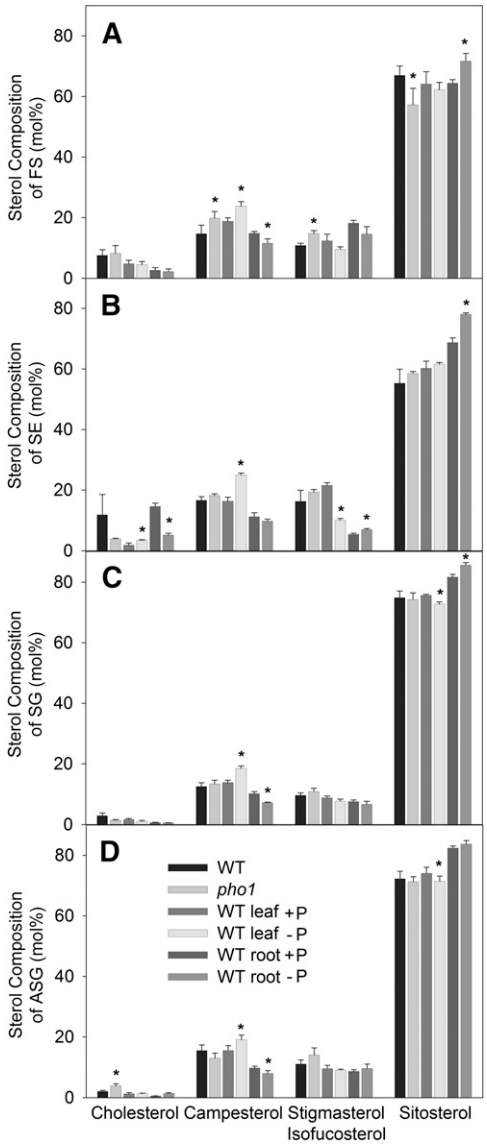

Fig. 9. Sterol composition of *Arabidopsis* leaves and roots measured by Q-TOF MS/MS. Lipids were extracted from *Arabidopsis* leaves of WT and *pho1* mutant plants grown on soil and from leaves and roots of WT plants grown on synthetic medium with or without phosphate. Bars show the sterol composition of free sterols (A), sterol esters (B), sterol glucosides (C), and acylated sterol glucosides (D). Data are means ± SD of five replicas. The results were confirmed by a second independent biological experiment. Sterol lipids containing stigmasterol or isofucosterol were not distinguished. Values that are significantly different from those of the WT or the phosphate-containing control and are higher than 2 mol% are indicated by an asterisk (according to Student's *t* test; $P < 0.02$).

strongly on the presence or absence of a double bond in the sterol moiety. The peak sizes of the sterol fragments were reduced for saturated SGs compared with those of unsaturated SGs. A correction factor was determined to compensate for the differences in fragmentation efficiency. Similarly, the abundance of the sterol fragment, F_S, of ASGs with saturated sterol moiety was much lower than that of ASGs with unsaturated sterol. The F_S peak of ASGs with saturated sterol moiety was therefore not suitable for

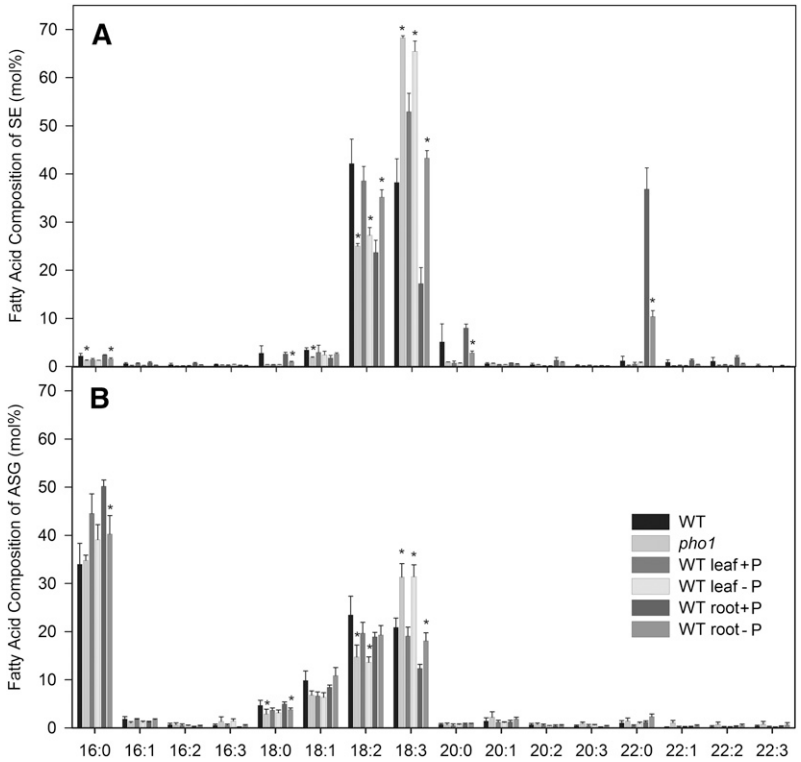

Fig. 10. Fatty acid composition of sterol esters and acylated sterol glucosides determined by Q-TOF MS/MS. A: Sterol esters; (B) acylated sterol glucosides. Sterol lipids were isolated from leaves of WT and *pho1* mutant plants grown on soil and from leaves and roots of WT plants grown on synthetic medium with or without phosphate. Bars show acyl composition as means ± SD of five measurements. Data were confirmed by a second independent biological experiment. Values that are significantly different from those of the WT or phosphate-containing control and higher than 2 mol% are indicated by an asterisk (according to Student's *t* test; $P < 0.02$).

quantification, and a different fragment, F_{AG}, corresponding to the acylated glucose head group was used. In the present study, saturated sterols (internal standards) and sterols containing one double bond at position 5 of the ring system (cholesterol, sitosterol, campesterol) or stigmasterol (one double bond at position 5, one double bond at position 22) were analyzed (Figs. 3, 4). Signal intensities for stigmasterol and sitosterol containing sterol lipids were very similar, indicating that the additional double bond at position 22 has a minor impact on ionization and fragmentation.

In agreement with previous studies (15, 49), sitosterol and campesterol were found to be the predominant sterol components in *Arabidopsis* leaves, as determined by Q-TOF MS/MS, while cholesterol, stigmasterol, and isofucosterol were minor components. Stigmasterol and isofucosterol are isomers with the same molecular formula ($C_{29}H_{48}O$). Conjugated lipids containing stigmasterol or isofucosterol give rise to isobaric fragments and therefore cannot be separated in MS/MS experiments.

Unsaturated acyl groups, mostly 18:2 and 18:3, were prevalent in SEs of leaves and roots (Fig. 4, 7). Interestingly, SEs from *Arabidopsis* roots contained a considerable amount of 22:0, which was absent from leaves. Roots are known to contain only small amounts of unsaturated fatty acids. The large amount of 22:0 in root SEs suggests that a considerable proportion of acyl groups in SEs was derived from the fatty acid elongation pathway at the endoplasmic reticulum. In contrast to SEs, saturated long chain fatty acids (16:0, 18:0) are prevalent in ASGs, equivalent to 40%–50% of all fatty acids of ASGs. In addition, smaller amounts of 18:1, 18:2, and 18:3 are found in ASGs.

The contents of sterol lipids obtained by Q-TOF MS/MS quantification were highly similar to the sterol lipid amounts measured by TLC/GC analysis (Fig. 7). Using a combination of TLC and GC, the contents of FS and SE in *Arabidopsis* leaves were previously determined as 1,021 and 174 μg g^{-1} dry weight (DW), respectively (49). This corresponds to 2.4 and 0.26 μmol g^{-1} DW, respectively. Higher values (~1,600 and 380 μg g^{-1} DW for FS and SE, respectively) were measured in a different study (11). Considering that the DW-to-FW ratio for *Arabidopsis* leaves is ~0.1, this translates into ~0.24–0.38 and 0.026–0.056 μmol g^{-1} FW for FS and SE, respectively, which is in the same range as the values of 0.33 and 0.036 μmol g^{-1} FW determined by Q-TOF MS/MS in this study (Fig. 7). The ratios of SG and ASG in *Arabidopsis* leaves relative to the other sterol lipids were previously calculated using the equations (SG + ASG)/FS = 0.15 and ASG/SE = 0.41 (15). These ratios are comparable to those calculated from Q-TOF MS/MS measurements, i.e., (SG + ASG)/FS = 0.14 and ASG/SE = 0.35 (Fig. 7).

The sterol composition percentages of *Arabidopsis* leaves were previously measured as 4, 16, 2, and 78% and 13, 12, 15, and 60% for cholesterol, campesterol, isofucosterol, and

sitosterol in FS and SE, respectively (49). These values are in accordance with those measured by Q-TOF MS/MS, 8, 15, 11, and 67% and 12, 17, 16, and 55% for cholesterol, campesterol, stigmasterol/isofucosterol, and sitosterol in FS and SE, respectively (Fig. 9). As indicated above, stigmasterol and isofucosterol cannot be separated by Q-TOF MS/MS.

Phosphate deficiency is known to cause a strong increase in the glycolipids DGDG and SQDG and a concomitant decrease in phospholipids. This adaptive process provides the means to save phosphate during growth on phosphate-limiting soils (2). SG and ASG also represent phosphate-free glycolipids and are localized to extraplastidial membranes, in particular to the plasma membrane. Previously, changes in plasma membrane lipid composition were recorded for oat roots (22, 24). After growth on phosphate-deficient medium, there was an increase in the proportion of SG and ASG relative to the total oat root plasma membrane lipids. Measurements of sterol lipids in *Arabidopsis* leaves and roots by Q-TOF MS/MS after phosphate deprivation were in agreement with the results previously obtained with oat. In leaves of the *pho1* mutant and the WT plants deprived of phosphate, SG and ASG were increased, while in roots, there were only minor changes in ASG. In addition, the SE content in leaves and roots was strongly increased during phosphate deprivation. The SE content was not determined during phosphate deprivation in oat, as it does not represent an authentic plasma membrane lipid (22, 24). Furthermore, the SE content in leaves of *Arabidopsis* plants grown on synthetic medium was elevated compared with that in plants grown on soil. Previous studies showed that the amount of SE in plants depends on the developmental stage, light conditions, and tissue type (51). In general, the amount of SE increases with plant age and during biotic and abiotic stress including senescence. It is believed that the accumulation of SE in oil bodies of leaf cells is in part due to the acylation of FS derived from the plasma membrane and thus represents a stress-related regulatory mechanism of membrane lipid homeostasis. For this reason, the increase of SE under conditions of phosphate deprivation or after transfer to synthetic medium presumably represents a general stress response, rather than a specific process related to nutrient availability.

The acyl compositions of SE and ASG were more susceptible to changes in phosphate supply than the sterol composition, which remained more or less unchanged. An increase of 18:3 with a concomitant decrease of 18:2 acyl chains in SE and ASG was observed in the *pho1* mutant and in WT leaves depleted of phosphate. In SEs of roots, the content of saturated very-long-chain fatty acids (20:0; 22:0) was decreased. This can be explained by an increased synthesis of SEs with 18:2 and 18:3 acyl chains.

Nanospray direct infusion Q-TOF MS with fragment-specific MS/MS experiments provides a robust and sensitive method for the quantification of sterol lipids. Signals for all sterol lipid classes were found to be linear over greater than 2 (ASG) and 3–4 (FS, SE, SG) orders of magnitude, which was sufficient to accurately quantify all molecular species of sterol lipids in *Arabidopsis* leaves. An important advantage of the Q-TOF method over classical TLC/GC-based protocols is the fact that detailed information on the molecular species composition of SEs and ASGs can be obtained. Furthermore, this method can easily be extended to measure sterol lipids in different tissues and in other plant species or organisms by adding further sterol-specific molecular species to the targeted MS/MS lists.

Nanospray ion sources are known to provide a strong increase in sensitivity compared with ESI. This is due in part to the fact that ionization efficiency is improved because of the reduced sizes of solvent droplets released during infusion and to the fact that a lower sample volume is required. In fact, all sterol lipid measurements by Q-TOF MS/MS could be done with a lipid extract derived from a single *Arabidopsis* leaf. The lower limit for accurate quantification of the molecular species of sterol lipids (Figs. 4 and 5) was in the range of 0.01 nmol in 200 µl of solvent by Q-TOF MS/MS. At a flow rate of 1 µl min^{-1}, a measuring time of 5 min (equivalent to 5 µl) usually is sufficient to perform the fragmentation experiments required for quantification of all sterol lipids. Therefore, the lower limit for quantification of molecular sterol lipid species is around 0.5 pmol. In comparison, the minimal amount of sterol lipid required for quantification by TLC and GC or by HPLC with an evaporative light-scattering detector lies in the low microgram (i.e., low nanomolar) range. Furthermore, the minimal amount of tissue required for Q-TOF MS/MS measurements of all four sterol lipid classes is only 20 mg compared with ~2 g required for TLC/GC quantification. Therefore, the Q-TOF-based method is far more sensitive than "classic" approaches of sterol lipid measurements. A further advantage of the Q-TOF method is the fact that it is much less labor intensive as it only requires SPE separation but is independent of TLC.

The sterol lipid quantification method was developed on a Q-TOF instrument equipped with a direct infusion nanospray ion source. Quantification was based on MS/MS experiments. The signal intensities for the characteristic fragments were electronically extracted from the spectra of all parental ions simulating neutral loss scanning experiments (e.g., for SG) or precursor ion scanning experiments (e.g., for betainylated FS). For this reason, the Q-TOF strategy of sterol lipid quantification can easily be transferred to other tandem mass spectrometers including triple-quadrupole instruments equipped with a nanospray or ESI source.

The authors thank Helga Peisker (University of Bonn) for technical assistance during Q-TOF measurements and Felix Lippold (University of Bonn) for support with data analysis.

REFERENCES

1. Joyard, J., M. A. Block, A. Malhèrbe, E. Maréchal, and R. Douce. 1994. Origin and synthesis of galactolipid and sulfolipid head groups *In* Lipid Metabolism In Plants. T. S. J. Moore, editor. CRC Press, Boca Raton (FL). 231–258.
2. Benning, C., and H. Ohta. 2005. Three enzyme systems for galactoglycerolipid biosynthesis are coordinately regulated in plants. *J. Biol. Chem.* **280:** 2397–2400.

3. Markham, J. E., and J. G. Jaworski. 2007. Rapid measurement of sphingolipids from *Arabidopsis thaliana* by reversed-phase high-performance liquid chromatography coupled to electrospray ionization tandem mass spectrometry. *Rapid Commun. Mass Spectrom.* **21:** 1304–1314.
4. Markham, J. E., J. Li, E. B. Cahoon, and J. G. Jaworski. 2006. Separation and identification of major plant sphingolipid classes from leaves. *J. Biol. Chem.* **281:** 22684–22694.
5. Benveniste, P. 2004. Biosynthesis and accumulation of sterols. *Annu. Rev. Plant Biol.* **55:** 429–457.
6. Fujioka, S., S. Takatsuto, and S. Yoshida. 2002. An early C-22 oxidation branch in the brassinosteroid biosynthetic pathway. *Plant Physiol.* **130:** 930–939.
7. Kemp, R. J., and E. I. Mercer. 1968. The sterol esters of maize seedlings. *Biochem. J.* **110:** 111–118.
8. Zinser, E., F. Paltauf, and G. Daum. 1993. Sterol composition of yeast organelle membranes and subcellular distribution of enzymes involved in sterol metabolism. *J. Bacteriol.* **175:** 2853–2858.
9. Banas, A., A. S. Carlsson, B. Huang, M. Lenman, W. Banas, M. Lee, A. Noiriel, P. Benveniste, H. Schaller, P. Bouvier-Navé, et al. 2005. Cellular sterol ester synthesis in plants is performed by an enzyme (phospholipid:sterol acyltransferase) different from the yeast and mammalian acyl-CoA:sterol acyltransferases. *J. Biol. Chem.* **280:** 34626–34634.
10. Chen, Q., L. Steinhauer, J. Hammerlindl, W. Keller, and J. Zou. 2007. Biosynthesis of phytosterol esters: identification of a sterol O-acyltransferase in *Arabidopsis*. *Plant Physiol.* **145:** 974–984.
11. Bouvier-Navé, P., A. Berna, A. Noiriel, V. Compagnon, A. S. Carlsson, A. Banas, S. Stymne, and H. Schaller. 2010. Involvement of the phospholipid sterol acyltransferase 1 in plant sterol homeostasis and leaf senescence. *Plant Physiol.* **152:** 107–119.
12. Grunwald, C. 1971. Effects of free sterols, steryl ester, and steryl glycoside on membrane permeability. *Plant Physiol.* **48:** 653–655.
13. Grille, S., A. Zaslawski, S. Thiele, J. Plat, and D. Warnecke. 2010. The functions of steryl glycosides come to those who wait: recent advances in plants, fungi, bacteria and animals. *Prog. Lipid Res.* **49:** 262–288.
14. Warnecke, D. C., M. Baltrusch, F. Buck, F. P. Wolter, and E. Heinz. 1997. UDP-glucose:sterol glucosyltransferase: cloning and functional expression in *Escherichia coli*. *Plant Mol. Biol.* **35:** 597–603.
15. DeBolt, S., W. R. Scheible, K. Schrick, M. Auer, F. Beisson, V. Bischoff, P. Bouvier-Navé, A. Carroll, K. Hematy, Y. Li, et al. 2009. Mutations in UDP-glucose:sterol glucosyltransferase in *Arabidopsis* cause transparent testa phenotype and suberization defect in seeds. *Plant Physiol.* **151:** 78–87.
16. Frasch, W., and D. Grunwald. 1976. Acylated steryl glycoside synthesis in seedlings of *Nicotiana tabacum* L. *Plant Physiol.* **58:** 744–748.
17. Warnecke, D., R. Erdmann, A. Fahl, B. Hube, F. Müller, T. Zank, U. Zähringer, and E. Heinz. 1999. Cloning and functional expression of UGT genes encoding sterol glucosyltransferases from *Saccharomyces cerevisiae*, *Candida albicans*, *Pichia pastoris*, and *Dictyostelium discoideum*. *J. Biol. Chem.* **274:** 13048–13059.
18. Griebel, T., and J. Zeier. 2010. A role for β-sitosterol to stigmasterol conversion in plant-pathogen interactions. *Plant J.* **63:** 254–268.
19. Wunder, C., Y. Churin, F. Winau, D. Warnecke, M. Vieth, B. Lindner, U. Zähringer, H-J. Mollenkopf, E. Heinz, and T. Meyer. 2006. Cholesterol glucosylation promotes immune evasion by *Helicobacter pylori*. *Nat. Med.* **12:** 1030–1038.
20. Oku, M., D. Warnecke, T. Noda, F. Müller, E. Heinz, H. Mukaiyama, N. Kato, and Y. Sakai. 2003. Peroxisome degradation requires catalytically active sterol glucosyltransferase with a GRAM domain. *EMBO J.* **22:** 3231–3241.
21. Dörmann, P., and C. Benning. 2002. Galactolipids rule in seed plants. *Trends Plant Sci.* **7:** 112–118.
22. Tjellström, H., L. I. Hellgren, A. Wieslander, and A. S. Sandelius. 2010. Lipid asymmetry in plant plasma membranes: phosphate deficiency-induced phospholipid replacement is restricted to the cytosolic leaflet. *FASEB J.* **24:** 1128–1138.
23. Christie, W., S. Gill, J. Nordback, Y. Itabashi, S. Sanda, and A. Slabas. 1998. New procedures for rapid screening of leaf lipid components from *Arabidopsis*. *Phytochem. Anal.* **9:** 53–57.
24. Andersson, M. X., K. E. Larsson, H. Tjellström, C. Liljenberg, and A. S. Sandelius. 2005. Phosphate-limited oat. The plasma membrane and the tonoplast as major targets for phospholipid-to-glycolipid replacement and stimulation of phospholipases in the plasma membrane. *J. Biol. Chem.* **280:** 27578–27586.
25. Wenk, M. 2005. The emerging field of lipidomics. *Nat. Rev. Drug Discov.* **4:** 594–610.
26. Welti, R., W. Li, M. Li, Y. Sang, H. Biesiada, H-E. Zhou, C. Rajashekar, T. Williams, and X. Wang. 2002. Profiling membrane lipids in plant stress responses. Role of phospholipase Dα in freezing-induced lipid changes in *Arabidopsis*. *J. Biol. Chem.* **277:** 31994–32002.
27. Devaiah, S. P., M. R. Roth, E. Baughman, M. Li, P. Tamura, R. Jeannotte, R. Welti, and X. Wang. 2006. Quantitative profiling of polar glycerolipid species from organs of wild-type *Arabidopsis* and a PHOSPHOLIPASE Da1 knockout mutant. *Phytochemistry.* **67:** 1907–1924.
28. Ejsing, C. S., J. L. Sampaio, V. Surendranath, E. Duchoslav, K. Ekroos, R. W. Klemm, K. Simons, and A. Shevchenko. 2009. Global analysis of the yeast lipidome by quantitative shotgun mass spectrometry. *Proc. Natl. Acad. Sci. U S A.* **106:** 2136–2141.
29. Karu, K., M. Hornshaw, G. Woffendin, K. Bodin, M. Hamberg, G. Alvelius, J. Sjövall, J. Turton, Y. Wang, and W. Griffiths. 2007. Liquid chromatography-mass spectrometry utilizing multi-stage fragmentation for the identification of oxysterols. *J. Lipid Res.* **48:** 976–987.
30. Liebisch, G., M. Binder, R. Schifferer, T. Langmann, B. Schulz, and G. Schmitz. 2006. High throughput quantification of cholesterol and cholesteryl ester by electrospray ionization tandem mass spectrometry (ESI-MS/MS). *Biochim. Biophys. Acta.* **1761:** 121–128.
31. Honda, A., K. Yamashita, H. Miyazaki, M. Shirai, T. Ikegami, G. Xu, M. Numazawa, T. Hara, and Y. Matsuzaki. 2008. Highly sensitive analysis of sterol profiles in human serum by LC-ESI-MS/MS. *J. Lipid Res.* **49:** 2063–2073.
32. Johnson, D. W., H. J. ten Brink, and C. Jakobs. 2001. A rapid screening procedure for cholesterol and dehydrocholesterol by electrospray ionization tandem mass spectrometry. *J. Lipid Res.* **42:** 1699–1705.
33. Jiang, X., D. Ory, and X. Han. 2007. Characterization of oxysterols by electrospray ionization tandem mass spectrometry after one-step derivatization with dimethylglycine. *Rapid Commun. Mass Spectrom.* **21:** 141–152.
34. Murashige, T., and F. Skoog. 1962. A revised medium for rapid growth and bio assays with tobacco tissue cultures. *Physiol. Plant.* **15:** 473–497.
35. Estelle, M. A., and C. Somerville. 1987. Auxin-resistant mutants of *Arabidopsis thaliana* with an altered morphology. *Mol. Gen. Genet.* **206:** 200–206.
36. Gaude, N., Y. Nakamura, W-R. Scheible, H. Ohta, and P. Dörmann. 2008. Phospholipase C5 (NPC5) is involved in galactolipid accumulation during phosphate limitation in leaves of *Arabidopsis*. *Plant J.* **56:** 28–39.
37. Delhaize, E., and P. J. Randall. 1995. Characterization of a phosphate-accumulator mutant of *Arabidopsis thaliana*. *Plant Physiol.* **107:** 207–213.
38. Hamburger, D., E. Rezzonico, J. MacDonald-Comber Petétot, C. Somerville, and Y. Poirier. 2002. Identification and characterization of the *Arabidopsis PHO1* gene involved in phosphate loading to the xylem. *Plant Cell.* **14:** 889–902.
39. Iga, D. P., S. Iga, R. R. Schmidt, and M-C. Buzasc. 2005. Chemical synthesis of cholesteryl beta-D-galactofuranoside and -pyranoside. *Carbohydr. Res.* **340:** 2052–2054.
40. Buseman, C. M., P. Tamura, A. A. Sparks, E. J. Baughman, S. Maatta, J. Zhao, M. R. Roth, S. W. Esch, J. Shah, T. D. Williams, et al. 2006. Wounding stimulates the accumulation of glycerolipids containing oxophytodienoic acid and dinor-oxophytodienoic acid in *Arabidopsis* leaves. *Plant Physiol.* **142:** 28–39.
41. Dörmann, P., S. Hoffmann-Benning, I. Balbo, and C. Benning. 1995. Isolation and characterization of an *Arabidopsis* mutant deficient in the thylakoid lipid digalactosyl diacylglycerol. *Plant Cell.* **7:** 1801–1810.
42. Schaller, H., B. Grausem, P. Benveniste, M-L. Chye, C-T. Tan, Y-H. Song, and N-H. Chua. 1995. Expression of the *Hevea brasiliensis* (H.B.K.) Müll. Arg. 3-hydroxy-3-methylglutaryl-coenzyme A reductase 1 in tobacco results in sterol overproduction. *Plant Physiol.* **109:** 761–770.
43. Li, Y. L., X. Su, P. D. Stahl, and M. L. Gross. 2007. Quantification of diacylglycerol molecular species in biological samples by electrospray ionization mass spectrometry after one-step derivatization. *Anal. Chem.* **79:** 1569–1574.
44. Vassel, B., and W. G. Skelly. 1963. N-Chlorobetainyl chloride. *Org Synth.* **4:** 154.
45. Ejsing, C. S., E. Duchoslav, J. Sampaio, K. Simons, R. Bonner, C. Thiele, K. Ekroos, and A. Shevchenko. 2006. Automated identification and quantification of glycerophospholipid molecular species by multiple precursor ion scanning. *Anal. Chem.* **78:** 6202–6214.

46. Brügger, B., G. Erben, R. Sandhoff, F. T. Wieland, and W. D. Lehmann. 1997. Quantitative analysis of biological membrane lipids at the low picomole level by nano-electrospray ionization tandem mass spectrometry. *Proc. Natl. Acad. Sci. U S A.* **94:** 2339–2344.
47. Han, X., and R. Gross. 2001. Quantitative analysis and molecular species fingerprinting of triacylglyceride molecular species directly from lipid extracts of biological samples by electrospray ionization tandem mass spectrometry. *Anal. Biochem.* **295:** 88–100.
48. Hutchins, P. M., R. M. Barkley, and R. C. Murphy. 2008. Separation of cellular nonpolar neutral lipids by normal-phase chromatography and analysis by electrospray ionization mass spectrometry. *J. Lipid Res.* **49:** 804–813.
49. Gachotte, D., R. Meens, and P. Benveniste. 1995. An *Arabidopsis* mutant deficient in sterol biosynthesis: heterologous complementation by *ERG3* encoding a Δ^7-sterol-C-5-desaturase from yeast. *Plant J.* **8:** 407–416.
50. Poirier, Y., S. Thoma, C. Somerville, and J. Schiefelbein. 1991. Mutant of *Arabidopsis* deficient in sylem loading of phosphate. *Plant Physiol.* **97:** 1087–1093.
51. Dyas, L., and L. Goad. 1993. Steryl fatty acyl esters in plants. *Phytochemistry.* **34:** 17–29.